Elsevier Editorial System(tm) for Experimental Parasitology

Manuscript Draft

Manuscript Number: EP-15-466R1

Title: Role of H+-pyrophosphatase activity in the regulation of intracellular pH in a scuticociliate parasite of turbot: physiological effects

Article Type: Research Paper

Keywords: Philasterides dicentrarchi; intracellular pH; calcium; ATP; H+-PPase; osmoregulation

Corresponding Author: Dr. Jose Manuel Leiro Vidal, Ph.D.

Corresponding Author's Institution: University of Santiago de Compostela

First Author: Natalia Mallo

Order of Authors: Natalia Mallo; Jesús Lamas; Ana Paula De Felipe; Rosa Ana Sueiro; Francisco Fontenla; Jose Manuel Leiro Vidal, Ph.D.

Abstract: The scuticociliatosis is a very serious disease that affects the cultured turbot, and whose causal agent is the anfizoic and marine euryhaline ciliate P. dicentarchi. Several protozoans possess acidic organelles that contain high concentrations of pyrophosphate (PPi), Ca2+ and other elements with essential roles in vesicular trafficking, pH homeostasis and osmoregulation. P. dicentrarchi possesses a pyrophosphatase (H+-PPase) that pumps H+ through the membranes of vacuolar and alveolar sacs. These compartments share common features with the acidocalcisomes described in other parasitic protozoa (e.g. acid content and Ca2+ storage). We evaluated the effects of Ca2+ and ATP on H +-PPase activity in this ciliate and analyzed their role in maintaining intracellular pH homeostasis and osmoregulation, by the addition of PPi and inorganic molecules that affect osmolarity. Addition of PPi led to acidification of the intracellular compartments, while the addition of ATP, CaCl2 and bisphosphonates analogous of PPi and Ca2+ metabolism regulators led to alkalinization and a decrease in H+-PPase expression in trophozoites. Addition of NaCl led to proton release, intracellular Ca2+ accumulation and downregulation of H+-PPase expression. We conclude that the regulation of the acidification of intracellular compartments may be essential for maintaining the intracellular pH homeostasis necessary for survival of ciliates and their adaptation to salt stress, which they will presumably face during the endoparasitic phase, in which the salinity levels are lower than in their natural environment.

Graphical Abstract

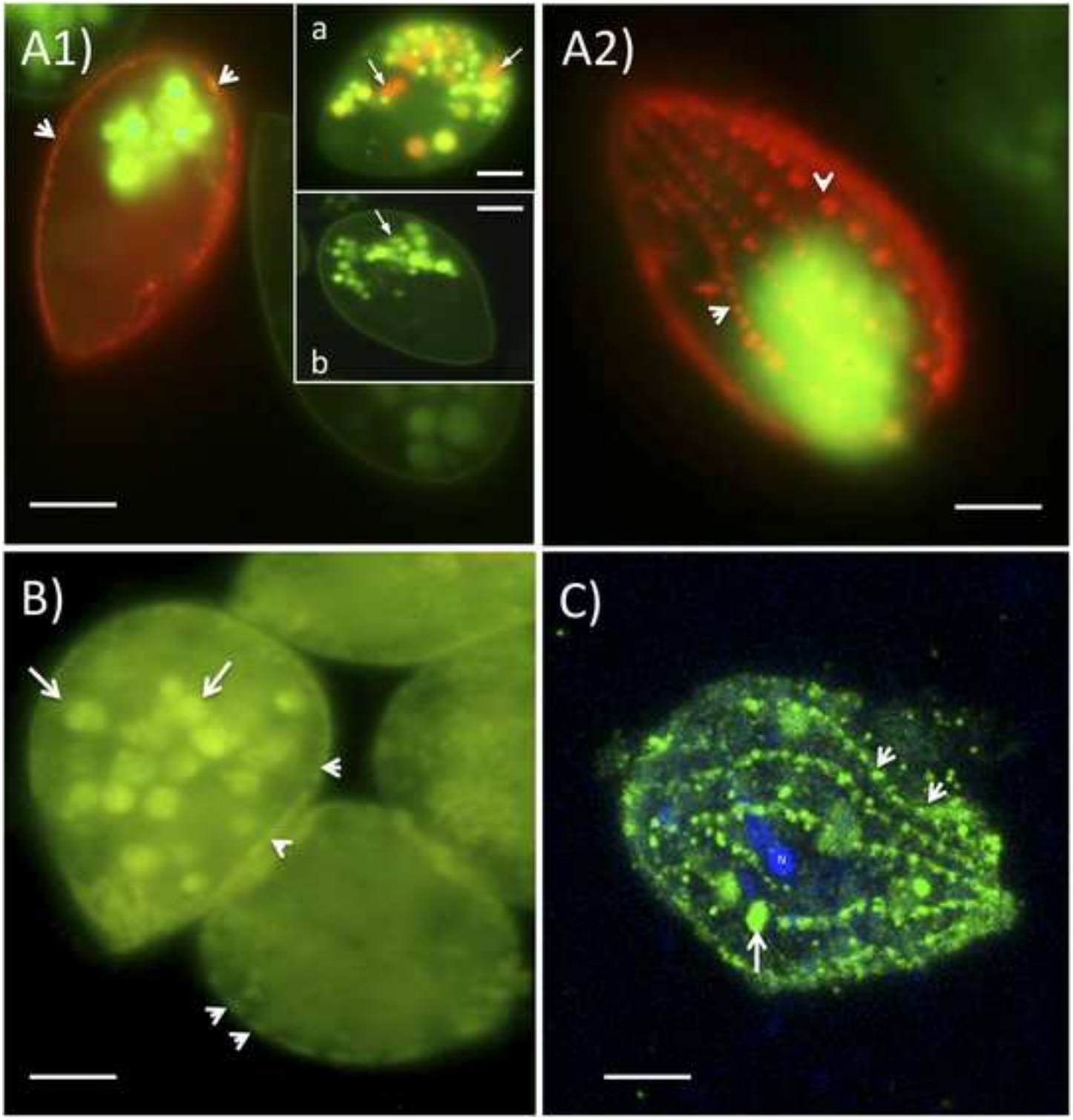

Highlights

- The existence of acidocalcisome-like structures in a ciliate parasite is proposed
- ATP and Ca^{2+} regulate the enzymatic activity of H^{+}-pyrophosphatase
- The regulation of intracellular pH is key to the survival of the parasite
- Disruption of pH homeostasis it can be a chemotherapeutic target

Role of H^+-pyrophosphatase activity in the regulation of intracellular pH in a scuticociliate parasite of turbot: physiological effects

Natalia Mallo[a], Jesús Lamas[b], Ana-Paula DeFelipe[a], Rosa-Ana Sueiro[a,b], Francisco Fontenla[b], José-Manuel Leiro[a,*]

[a]*Laboratorio de Parasitología, Instituto de Investigación y Análisis Alimentarios, Universidad de Santiago de Compostela, Santiago de Compostela, Spain.*

[b]*Departamento de Biología Celular y Ecología e Instituto de Acuicultura, Facultad de Biología, Universidad de Santiago de Compostela, Santiago de Compostela, Spain.*

Short title: Intracellular pH homeostasis and osmoregulation in a scuticociliate parasite

*Corresponding author:

José M. Leiro, Laboratorio de Parasitología, Instituto de Investigación y Análisis Alimentarios, c/ Constantino Candeira s/n, 15782, Santiago de Compostela (A Coruña), Spain; Tel: 34981563100; Fax: 34881816070; E-mail: josemanuel.leiro@usc.es

Abstract

The scuticociliatosis is a very serious disease that affects the cultured turbot, and whose causal agent is the anfizoic and marine euryhaline ciliate *P. dicentarchi*. Several protozoans possess acidic organelles that contain high concentrations of pyrophosphate (PPi), Ca^{2+} and other elements with essential roles in vesicular trafficking, pH homeostasis and osmoregulation. *P. dicentrarchi* possesses a pyrophosphatase (H^+-PPase) that pumps H^+ through the membranes of vacuolar and alveolar sacs. These compartments share common features with the acidocalcisomes described in other parasitic protozoa (e.g. acid content and Ca^{2+} storage). We evaluated the effects of Ca^{2+} and ATP on H^+-PPase activity in this ciliate and analyzed their role in maintaining intracellular pH homeostasis and osmoregulation, by the addition of PPi and inorganic molecules that affect osmolarity. Addition of PPi led to acidification of the intracellular compartments, while the addition of ATP, $CaCl_2$ and bisphosphonates analogous of PPi and Ca^{2+} metabolism regulators led to alkalinization and a decrease in H^+-PPase expression in trophozoites. Addition of NaCl led to proton release, intracellular Ca^{2+} accumulation and downregulation of H^+-PPase expression. We conclude that the regulation of the acidification of intracellular compartments may be essential for

maintaining the intracellular pH homeostasis necessary for survival of ciliates and their adaptation to salt stress, which they will presumably face during the endoparasitic phase, in which the salinity levels are lower than in their natural environment.

Keywords: *Philasterides dicentrarchi*; intracellular pH; calcium; ATP; H^+-PPase; osmoregulation.

1. Introduction

Philasterides dicentrarchi, a marine euryhaline scuticociliate, is a facultative parasite initially described in cultured European seabass *Dicentrarchus labrax* (Dragesco et al., 1995) and which causes serious mortalities in cultured turbot *Scophthalmus maximus* (Iglesias et al., 2001). Like other ciliates, this species displays a high capacity to adapt to changes in environmental osmolarity (Kaneshiro et al., 1969). Maintenance of cell volume is a fundamental mechanism of cellular homeostatic that must have arisen very early on in the evolution of cells (Maroulis et al., 2003). Parasitic protozoans have developed several mechanisms to adapt to osmotic stress and possess two organelles with an essential role in these adaptations: the acidic organelles acidocalcisomes and the contractile vacuole complex (Rohloff and Docampo, 2008). The main function of acidocalcisomes is storage of H^+ and phosphorus, for use in pyrophosphate (PPi) and polyphosphate (PolyP) metabolism, osmoregulation and maintenance of pH and Ca^{2+} homeostasis (Docampo and Moreno, 2001; Moreno and Docampo, 2009; Docampo and Moreno 2011; Docampo et al., 2013; Li et al., 2014). Acidocalcisomes share some properties with plant vacuoles and have several pumps in their membranes. Two of these pumps (V-H^+-PPase and V- H^+-ATPase) are H^+

translocases (Hannaert *et al*., 2003), which participate in the conservation of acidic conditions required for Ca^{2+} retention (García *et al.*,1998; Bonansea *et al*., 2012). Several pumps such as H^+-PPase, H^+-ATPase, Na^+/H^+ and $Ca^{2+/}H^+$ exchangers and Ca^{2+}-ATPase participate in or interfere with pH maintenance (Luo *et al.,* 2001; Rodrigues *et al*., 2002; Saliba *et al.,* 2003; Docampo *et al*., 2005).

In *Paramecium*, staining of acid compartments with pH sensitive fluorescent dyes has revealed the distribution of several acidic vesicles in the cellular cytoplasm and some acidosomes close to the cytostome (Wassmer *et al.,* 2009). The presence of granules containing Ca^{2+} and Mg_2PPi has been reported in another ciliate, *Tetrahymena pyriformis* (Heinonen, 2003). The possibility that ciliates possess acidocalcisomes is suggested by the fact that they contain many proteins that are activated by Ca^{2+}, particularly in the cortex and cilia (Kim et al., 2002; Kissmehl et al., 2006); however, these proteins have not yet been characterized in *Philasterides*.

In ciliates, the alveolar sacs are distributed along the inner side of the membrane, which is covered by locomotive cilia (Lynn and Corliss, 1991). As the entire cell is coated by cilia, substantial amounts of Ca^{2+} are required for ciliary motility and for intra- and extracellular signalling. The Ca^{2+} of alveolar sacs of ciliates, which have been identified as Ca^{2+} stores, is actively imported inside the alveoli, in an ATP and Mg^{2+}-dependent process (Stelly *et al*., 1995; Sahoo *et al*., 2004; Plattner, 2014; 2015). In *P. dicentrarchi,* the alveolar sacs are of variable size, possibly reflecting changes in osmotic or ionic concentration across the membrane in response to environmental conditions (Paramá et al., 2006); the membranes of vacuoles and alveolar sacs of trophozoites possess H^+-PPase, a enzyme typically present in the acidocalcisomes of protozoan parasites (Mallo et al., 2015; 2016a).

In this study, we investigated the potential presence of acidocalcisome-like organelles in the scuticociliate *P. dicentrarchi* and analyzed the role of adenosine triphosphate (ATP) and Ca^{2+} on intracellular acidification, H^+ translocating activity and H^+-PPase expression. We also evaluated the effect of osmolarity on the levels of expression of this enzyme, assessing the physiological implication of acidic intracellular compartments in osmoregulation of the ciliate.

2. Material and Methods

2.1. Experimental animals and parasites

Specimens of turbot, *Scophthalmus maximus*, of approximately 50 g body weight were obtained from a fish farm in Galicia. The fish were placed in 250L tanks with recirculating seawater at 17-18ºC under a photoperiod of 12h light/dark, and they were fed daily with commercial pellets (Skretting, Burgos, Spain). Before starting the experiments, fish were acclimated to the laboratory conditions for 2 weeks.

ICR CD-1 mice (Swiss) of age 8-10 weeks were purchased from Charles River Laboratories (U.S.A.) for use in the experiments. All experiments were carried out following the European Regulations on Animal Protection (Directive 86/609), the Declaration of Helsinki and/ or the Guide of Care and Use of Laboratory Animals adopted by the US National Institutes of Health (NIH). All experimental protocols were approved by the Institutional Animal Care and Use Committee of the University of Santiago de Compostela.

We obtained naturally infected turbot, showing signs of scuticociliatosis, from a fish farm in Galicia (NW Spain). Specimens of the ciliate *P. dicentrarchi* (isolate I1;

Budiño *et al.*, 2011) were obtained aseptically from intraperitoneal cavity ascites of these turbot, as previously described (Iglesias *et al.*, 2001). The ciliates were grown at 21° C in complete sterile L-15 medium (Leibovitz, PAA Laboratories GmbH, 10% salinity, pH 7.2) containing 90 mg/L of adenosine, cytidine and uridine, 150 mg/L guanosine, 5 g/L glucose, 400 mg/L of L-α-phosphatidylcholine, 200 mg/L Tween 80, 10% foetal calf serum, heat inactivated (FCS), and 10 mL/L of a solution containing antibiotics and antimycotics (100X) (100 units/ml penicillin G, 0.1 mg/mL streptomycin sulphate and 0.25 mg/mL amphotericin B; Sigma-Aldrich), as previously described (Iglesias *et al*., 2003). In some experiments, ciliates were grown in solutions of NaCl at the required concentration and with 10% FBS. In order to maintain the virulence of the ciliates, experimental infections were induced every 6 months by intraperitoneal injection of 200 µL of sterile physiological saline solution containing $5x10^5$ ciliates. Ciliates were recovered from ascites fluid, as previously described (Paramá *et al*., 2003; Leiro *et al*., 2008).

2.2. pH sensitive fluorescent staining

Ciliates (2.5×10^5) were permeabilized with digitonin (DIG) to a final concentration of 6.6 µM and washed twice with PBS by centrifugation before being stained with a solution of 3 µM acridine orange (Sigma-Aldrich) or with 75 nM Lysotracker Red DND -99 solution (Life Technologies) (both fluorophores that accumulate selectively in acidic compartments) for 10 min. In some experiments, ciliates also incubated with 0.1 mM of the PPi analogous pamidronate (PAM, Sigma-Aldrich). The stained ciliates were observed in a fluorescence or in a confocal microscope with an excitation BP 546 nm dichroic mirror filter and FT 580 nm LP

emission 590 nm filter (for acridine orange) and a BP 450-490 nm filter and FT 510 nm and LP 520 nm filter (for Lysotracker Red DND-99).

2.3. Location and quantification of intracellular Ca^{2+}

Ciliates (2.5×10^5), permeabilized with DIG as described above, were washed twice with HBSS, by centrifugation, and resuspended in assay medium (1X HBSS, 20 mM HEPES and 2.5 mM probenecid) to a final concentration of 1.25×10^6 ciliates/mL. The Ca^{2+} probe Fluo-4 NW (No-Wash, Fluo-4 NW Calcium Assay kit, Life Technologies) was added following manufacturer's instructions, and the fluorescence (Ex: 494nm, Em: 516nm) was visualized by fluorescence microscopy (Zeiss Axioplan, Germany).

For quantification of intracellular Ca^{2+}, the ciliates were washed twice, by centrifugation, and resuspended in assay medium to a final concentration of 1.25×10^6 ciliates/mL. The ciliates were then incubated with different treatments for 1 hour in 96-well microplates at 21° C. The cell-permeable Ca^{2+} indicator probe, Fluo-4 NW, was added following the manufacturer's instructions, and the fluorescence (Ex: 494nm, Em: 516nm) was measured in a fluorimeter (*FLx800*, BioTek USA). Negative controls without Ca^{2+} probe Fluo-4 NW were established (Takahashi *et al.*, 1999; Paredes *et al.*, 2008; Friedrich *et al.*, 2014).

2.4. Production of recombinant H^+-PPase of *P. dicentrarchi* in yeast cells

The total RNA in *P. dicentrarchi* was purified with a Nucleospin RNA kit (Macherey-Nagel, Düren, Germany), following the manufacturer's instructions. RNA was treated with DNAse I (DNAse I, RNAse free, Thermo Scientific) and the

concentration and purity were estimated in a NanoDrop ND-1000 spectrophotometer (NanoDrop Technologies, USA) by measurement at 260nm.

cDNA (25 µl/reaction) was synthesized with 1.25 mM random primer (Roche), 250µM of each deoxynucleoside triphosphate (dNTPs), 10mM dithiothreitol (DTT), 20U of RNAse inhibitor, 2.3mM $MgCl_2$ and 200U of reverse transcriptase of Moloney murine leukemia virus, (MMLV) (Promega), in buffer containing 30 mM Tris, 20 mM KCl (pH 8.3) and 2 µg RNA samples.

The PCR was carried out with gene-specific primers designed from a partial sequence of an H^+-PPase of *P. dicentrarchi* (Mallo *et al.*, 2015) (forward/reverse primer pair 5'-AAAGAAGAAGGGGTACCTTTGGATAAAAGAattgatgtcaacgccccctt-3' / 5'-TGGGACGCTCGACGGATCAGCGGCCGCTTAGTGGTGGTGGTGGTGGTGgggac cagaggtatctttta-3'). The primers were designed and optimized using the *Saccharomyces* Genome Database (http://www.yeastgenome.org/) by including a hybridization region with the yeast YEpFLAG-1 plasmid (Eastman Kodak Company) (upper case letters) and a poly His region. The PCR reaction was performed as previous described: 95 °C for 5 min, 30 cycles of 94 °C for 1 min, 55 °C for 1.5 min and 72 °C for 2 min followed by a 7-min extension phase at 72 °C. PCR products were purified with the Gene Jet PCR Purification Kit (Fermentas, Life Sciences) according to the manufacturer's instructions.

PCR purified products were cloned in the yeast expression vector YEpFLAG-1 (Eastman Kodak Company). This vector has a gene (TRP1) that completes tryptophan auxotrophy in the host cell (López-López *et al.*, 2010). *Saccharomyces cerevisiae* cells (strain BJ 3505) were transformed by the lithium acetate method (Ito *et al.*, 1983), with the YEpFLAG-1 linearized plasmid and EcoRI and SalI (Takara) digestion. The procedure involves co-transformation of yeast cells with the linearized empty plasmid

and the PCR-generated DNA fragment so that a recombination process occurs within the cell yielding a plasmid bearing the desired insert. Positive clones were selected using a free tryptophan complete medium (CM-Trp) containing glucose (20g/L), Yeast Nitrogen Base without amino acids (Sigma-Aldrich), adenine (40mg/L) and amino acids (40 mg/L each of histidine, leucine and tyrosine; 10 mg/L each of arginine, methionine and threonine 10mg/L; 60 mg/L of isoleucine and 40 mg/L of phenylalanine). Plasmidic DNA was purified with the Easy Yeast Plasmid Isolation Kit (Clonetech), following the manufacturer's instructions, and was analyzed by sequencing (Sistemas Genómicos, Spain).

The *P. dicentrarchi* recombinant protein (rH^+-PPase) was purified from transformed *Saccharomyces cerevisiae* cultures after 72 hours of growth in Yeast Peptone High Stability Expression Medium (an expression medium containing 1% glucose, 3% glycerol, 1% yeast extract and 8% peptone and that yields high plasmid stability), at 30ºC in an Erlenmeyer flask filled to approximately 20% of its volume with culture medium, with shaking at 250rpm (López-López, *et al*., 2010). A suitable volume of a pre-culture was added as the inoculum to yield an initial OD_{600} of 0.1. The cell suspension was centrifuged at 7500 x *g* for 15 min and the cleared supernatant was purified by immobilized metal affinity chromatography on a pre-charged Ni-Sepharose Histrap column (ÄKTAprime plus, GE Healthcare Life Sciences), which was initially equilibrated with 25 mL of binding buffer (20 mM Na_2HPO_4, 0.5 M NaCl, 20 mM imidazole, pH 7.4). After equilibration, 100mL of the culture medium containing the protein was charged through the column, and the protein bound to the column was finally eluted in 10 mL of elution buffer (20 mM Na_2HPO_4, 0.5 M NaCl, 250 mM imidazole, pH 7.4) (Mallo *et al.*, 2015). Elution fractions were collected and dialyzed overnight in 2 L of bidistilled water. The dialyzed sample was concentrated in an

Amicon Ultra centrifugal filter device (Millipore, USA) with a 10-kDa cut-off membrane before being analyzed in a 12.5% SDS-PAGE. The final protein concentration was calculated by the Bio-Rad Protein Assay, based on the Bradford method (Bradford, 1976).

2.5. Immunization and serum extraction

A group of five ICR (Swiss) CD-1 mice were immunized by i.p. injection with 200 µL per mouse of a 1:1 (v/v) mixture of Freund complete adjuvant (Sigma-Aldrich) and a solution containing 500 µg of purified rH^{+}-PPase. The same dose of purified protein was prepared in Freund's incomplete adjuvant and injected i.p in mice 15 and 30 days after the first immunization. The mice were bled via retrobulbar venous plexus 7 days after the secondary immunization (Piazzon et al., 2011) and the blood was left to coagulate overnight at 4º C before the serum was separated by centrifugation (2000 × g for 10 min), mixed 1:1 with glycerol and stored at −20ºC until use.

2.6. Transmission electronic microscopy (TEM)

Ciliates were collected by centrifugation at 1000 x *g* for 5 min. After fixation in 2.5% (v/v) glutaraldehyde in 0.1 M cacodylate buffer at pH 7.2, the ciliates were then washed several times with 0. 1 M cacodylate buffer, post-fixed in 1% (w/v) OsO4, pre-stained in saturated aqueous uranyl acetate, dehydrated through an acetone series and embedded in Spurr's resin. Semi-thin sections were then cut with an ultratome (Reichart-Jung, Ultracut E, Austria) and stained with 1% toluidine blue for examination in a light microscope. Ultrathin sections were stained in alcoholic uranyl acetate and lead citrate and viewed in a Philips CM12 transmission electron microscope (Philips, Eindhoven, Netherlands) at an accelerating voltage of 80 kV (Paramá *et al.*, 2006).

237

238 2.7. Measurement of PPi-dependent H^+-translocation

239 The fluorimetric test was carried out with acridine orange (a fluorescent cationic
240 dye which is accumulated in acidic compartments) as an indicator of transmembrane pH
241 difference in permeabilized ciliates (Rohloff and Docampo, 2006).

242 Ciliates (2.5 x 10^5) were permeabilized with DIG as described above, and
243 washed twice with PBS by centrifugation. They were then resuspended in assay buffer
244 containing 100 mM KCl, 0.4M glycerol, 1 mM Tris-EGTA, and 5mM Tris-HCl, 1 mM
245 PMSF and 1 ug/ml leupeptin (pH 8) and 2.5 µM acridine orange. The reaction was
246 initiated by the addition of Tris-PPi (1 mM) to medium containing 1.3 mM $MgSO_4$. The
247 kinetics of the decay in fluorescence was measured at 485/530 excitation /emission in a
248 fluorimeter (*Fluox800*, BioTek, USA) (Zhen *et al*, 1997; Hill *et al.*, 2000; Marchesini *et*
249 *al.*, 2000; Rodrigues *et al.*, 2000; Mallo *et al.*, 2015). In all cases, a negative control
250 without pyrophosphate was established. The compounds used were added from stock
251 solutions prepared in reaction buffer (Moreno *et al*., 2011). Because it acts as
252 alkalinizer, NH_4Cl was added in a final control test, to confirm that the decrease in
253 acridine orange fluorescence was due to accumulation in acidic compartments
254 (Rodrigues *et al*., 1999b; Lemercier *et al.*, 2002).

255

256 2.8. Immunofluorescence assay

257 For immunolocalization of H^+-PPase, an immunofluorescence assay was performed
258 following the protocol described previously (Mallo et al., 2015). Briefly, 5x10^6 ciliates were
259 centrifuged at 750 x *g* for 5 min, washed twice with Dulbecco's phosphate buffered saline
260 (DPBS, Sigma Aldrich) and fixed for 5 min in a solution of 4% formaldehyde in DPBS.
261 Following fixation, ciliates were washed twice with DPBS, resuspended in a solution containing

0.1% Triton X-100 (PBT) for 3 min and then washed twice with DPBS. Ciliates were then incubated with 1% bovine serum albumin (BSA) for 30 min. After blocking, ciliates were incubated at 4ºC overnight with a solution containing 1:100 dilutions of anti-rH^{+}-PPase form recombinant yeast antibody. Then, ciliates were washed 3 times with DPBS followed by 1 h incubation, at room temperature; with a 1:100 dilution of FITC conjugated rabbit anti-mouse IgG-FITC antibody (Sigma). After three in DPBS, the samples were double stained with 0.8 mg/mL 4', 6-diamidine-2-phenylindole (DAPI; Sigma-Aldrich) in DPBS for 15 min at room temperature (Paramá *et al.*, 2007). After three washes with DPBS samples were mounted in PBS-glycerol (1:1) and visualized by confocal microscopy (Leica TCS-SP2, LEICA Microsystems Heidelberg GmbH, Mannheim, Germany).

2.9. SDS-PAGE electrophoresis and Western blot

Enriched vesicle fractions (EVF) of the ciliates cultured for 6 hours with different treatments (no treatment, 1m MATP or 0.8mM $CaCl_2$) were obtained from 2.5×10^5 trophozoites for each preparation. Ciliates were centrifuged and washed twice in PBS and once with assay buffer (100 mM KCl, 0.4 M glycerol, 1 mM Tris–EGTA and 5 mM Tris–HCL, pH 8.0) containing 1 mM PMSF and 1 μg/mL leupeptin. The cell pellet was homogenized in a Potter S homogenizer (Braum Biotech, USA) until lysis was greater than 90% (generally 30 s). The mixture was resuspended in 5 mL of assay buffer and centrifuged once at 750 g for 5 min (to remove unbroken cells). The resulting supernatant was centrifuged at 15 000 g for 10 min, and the pellet was resuspended in PBS with loading buffer (without DTT) (Mallo *et al.*, 2015). Samples were separated by SDS-PAGE in 12.5% linear gels under non-reducing conditions. After electrophoresis, the gels were stained with Coomassie blue (Thermo Scientific Protein GelCode Blue Safe Stain; Thermo Fisher, USA) to determine the concentration of protein in each sample (Piazzón *et al*., 2008).

Simultaneously, one of the gels was transferred to a polyvinylidene fluoride (PVDF) membrane, at 15V for 35 min (0.45 · m, Millipore, USA) on a Trans-Blot SD transfer cell (Bio-Rad, USA. UU) embedded in transfer buffer containing 48 mM Tris, 29 mM glycine, 0.037% SDS and 20% methanol, pH 9.2. Membranes were stained with Ponceau S to verify transfer and incubated for 1.5 h at room temperature in Tris Buffer Saline (TBS; 50 mM Tris, 0.15 M NaCl, pH 7.4) containing 0.2% Tween 20 and 3% BSA. The membranes were then washed with TBS and incubated overnight at 4 °C with anti-H^+-PPase form recombinant yeast antibody at a ratio of 1:100. The membranes were incubated for 1 hour at room temperature with the secondary antibody (goat anti-mouse Ig antibody, 1:1000, Dakopatts) and visualized with a chemiluminescent substrate based on luminol (ECL Western Blotting Substrate Pierce, Thermo Scientific, USA). Membranes were photographed with a FlourChem® FC2 imaging system (Alpha Innotech, USA). Band intensity was analyzed using the Total Lab image master program (Mallo *et al.*, 2015).

2.10. Extraction of total RNA, reverse transcription and real-time polymerase chain reaction (qPCR)

Trophozoites were incubated for 2 hours with the different treatments (4, 8 and 37‰ NaCl, 1mM ATP 1mM and 0.8 mM $CaCl_2$). The total RNA from 10^7 cells/sample was isolated, treated with DNAse I and used to generate cDNA, as already described. The qPCR reaction was performed with a reaction mixture already containing the assay buffer and dNTPs, Maxima SYBR Green qPCR Master Mix (Thermo Scientific). The primer pair for the genes under study was used at a final concentration of 300 nM, and 1µl of cDNA was added per well. The volume was completed with RNase free distilled H_2O to a final reaction volume of 10 µL/well. The mixtures were heated at 95 °C for 5

min, followed by 40 cycles of 10s at 95 °C and 30s at 60 °C. At the end of the process, melting curve analysis was carried out at 95 °C for 15s, 55 °C for 15 s and 95 °C for 15 s. The specificity and the size of the PCR products obtained were confirmed by agarose gel electrophoresis at 2%. All reactions were carried out in a real time PCR system, Eco Real-time PCR system (Illumina). The relative quantification of gene expression was determined by the $2^{-\Delta\Delta Cq}$ method (Livak and Schmittgen, 2001), and the programme was used in accordance with minimum information guidelines for publishing real-time quantitative PCR experiments (Bustin *et al.*, 2009). The following primer sequences of H^+-PPase gene were used: forward/reverse, 5'-GCCTACGAAATGGTCGAAGA-3'/5'-GCATCGGTGTATTGTCCAGA-3'. Gene expression was normalized with the β-tubulin reference gene from *P. dicentrarchi* (forward/reverse primer sequence, 5′-ACCGGGGAATCTTAAACAGG-3′/5′-GCCACCTTATCCGTCCACTA-3′) and the normalized data were expressed in relative arbitrary units. The values show the mean ± the standard error (SE) of three trials.

The primer pairs were designed and optimized with the Primer 3 Plus programme (http://www.bioinformatics.nl/cgibin/primer3plus/primer3plus.cgi) with a Tm of 60 °C.

2.11. Statistical analysis

Results shown in the figures are expressed as means ± standard error. Significant differences ($P = 0.05$) were determined by analysis of variance (ANOVA) followed by Tukey – Kramer multiple comparisons test.

3. Results

337 3.1. Presence of Ca^{2+} and H^{+}-PPase in acidic intracellular compartments

338 Staining with the pH sensitive fluorescent dyes acridine orange and Lysotracker
339 Red DND-99 (Fig 1, A1 and A2) revealed intracellular acidic compartments in DIG-
340 permeabilized *P. dicentrarchi* trophozoites. Some important differences were observed
341 in the staining patterns of ciliates from the same culture batch. Some trophozoites
342 showed intense red fluorescent staining (acid pH) in the alveolar sacs, while others
343 showed only weak green florescent staining (alkaline pH), which was most evident in
344 the endocytic vacuoles (Fig. 1, A1). In the preparations stained only with acridine
345 orange, some DIG-permeabilized trophozoites stained various colours
346 (green/yellow/orange-red), indicating varying levels of pH in the endocytic vacuoles,
347 ranging from alkaline (green fluorescence) to acidic (orange/red fluorescence) (Fig. 1,
348 A1-a); however, when trophozoites are incubated with the bisphosphonate calcium
349 metabolism regulator PAM, a complete alkalinization of endocytic vacuoles is produced
350 (Fig. 1, A1-b). Likewise, the distribution of acidic alveolar sacs coincides with the
351 distribution of cilia (Fig. 1, A2).

352 In the trophozoites, Ca^{2+} was primarily located in the alveolar sacs and some
353 internal vacuoles (Fig. 1B). The staining patterns obtained with acid dyes and the Ca^{2+}
354 probe were both consistent with the pattern of immunostaining obtained using a
355 recombinant anti-H^{+}-PPase, with labelling of both internal vacuoles and alveolar sacs
356 located under the kinetia (Fig. 1C).

357 Examination by electron microscopy revealed spherical electro-dense structures
358 inside the alveolar sacs and also spread through the cytoplasm in the interior of the
359 cytoplasmic vacuoles (Fig. 2A). At the ultrastructural level, a close association between
360 the inner membrane of alveolar sacs and the immediately underlying mitochondria was
361 observed (Fig. 2B).

362

363 3.2. Regulatory effect of ATP and Ca^{2+} on the H^+-translocating activity

364 An assay of proton pumping activity was performed to investigate the effect of
365 PPi and ATP on H^+-translocation activity and acidification of intracellular
366 compartments, including the alveolar sacs, in *P. dicentrarchi*. Addition of PPi to DIG-
367 permeabilized trophozoites induced translocation of H^+ and the acidification of
368 intracellular compartments (Fig. 3A); however, the presence of ATP (0.01, 0.25, 0.5 and
369 1 mM) did not affect intracellular acidification, indicating that ATP does not stimulate
370 H^+-translocation (Fig. 3B). In samples in which PPi-driven H^+ translocation was
371 observed, this activity was inhibited by addition of 0.5 or 1 mM ATP (Fig. 3 C),
372 producing intracellular alkalinization. Addition (via a stock solution of 0.8 mM $CaCl_2$)
373 of Ca^{2+}(a known H^+-PPase inhibitor), or the bisphosphonate analogous PAM at 0.1 mM,
374 inhibited the H^+-translocating activity (Fig. 3D).

375

376 3.3. Role of ATP and Ca^{2+} in H^+-PPase protein and gene expression

377 Western blots of the vesicle-enriched fractions treated with Ca^{2+} (0.8mM $CaCl_2$)
378 and 1mM ATP revealed a significant decrease in the band intensity, measured by
379 densitometry software program, indicating a decrease in H^+-PPase expression relative to
380 the untreated controls (Fig. 4 A, B).

381 The relative H^+-PPase gene expression in *P. dicentrarchi* was quantified by RT-
382 qPCR of cDNA from ciliates cultivated with the different treatments for 2 hours. Both
383 treatments ($CaCl_2$ and ATP) induced a significant decrease in H^+-PPase expression (Fig.
384 4C).

385

386 3.4. Effects of salinity on H^+ translocating activity and intracellular Ca^{2+} levels

NaCl and KCl were used as sources of Na^+ and K^+, both of which are present in seawater, to study the effects of salinity on the H^+ translocation activity in *P. dicentrarchi*. H^+ pumping activity was induced by adding PPi in different buffers during sample preparation and, in one of these, NaCl replaced the KCl in the standard translocation assay buffer (100 mM KCl, 0.4 M glycerol, 1 mM Tris-EGTA, and 5mM Tris-HCl, 1 mM PMSF and 1μg/ml leupeptin, pH 8), at the same concentration (100 mM). Acidification only occurred when buffer containing KCl was used, and NaCl had an inhibitory effect on the H^+ translocation activity (Fig. 5A). With the aim of reversing the effect of NaCl, the same concentration of KCl was added, in an attempt to induce H^+ translocation. However, the activity was not recovered. When NaCl was added to the sample displaying H^+ pumping activity that was prepared in buffer containing KCl, addition of NaCl again resulted in alkalinization.

To analyze the effect of salinity and PPi on intracellular Ca^{2+} levels, ciliates were cultured for 24 hours in saline solutions of 4 and 8 ‰, conditions considered hypo-osmotic for these marine ciliates whose natural osmolarity is the 37 ‰. After the DIG-permeabilization and the addition of 1 mM PPi, the ciliates were incubated for 30 min. The Ca^{2+} probe (Fluo-4 NW) was then added and the fluorescence (Ex: 494nm, Em: 516nm) was measured after 1 hour. Addition of PPi caused a significant decrease in internal Ca^{2+} levels in both cases (Fig. 5B). The Ca^{2+} levels were lower under hypo-osmotic conditions (Fig. 5B)

4. Discussion

Ciliates are among the most abundantly distributed protozoa in the marine environment, and around 60 scuticociliate species have been described (Wang *et al.*, 2008). The capacity of ciliates to adapt to changes in salinity and pH is essential to

412 enable littoral colonization (Nisbet, 1984). Vacuoles and other acidic organelles play an
413 essential role in this capacity, including storage, sequestration of toxic compounds and
414 maintenance of turgor (Pittman *et al*., 2011). Studies of plant vacuoles have shown that
415 regulation of vacuole acidification is crucial for secretory and endocytic routes
416 (Baltscheffsky *et al*., 1999; Gaxiola *et al*., 2007). Moreover, pH homeostasis in
417 intracellular compartments is essential under pathological conditions, and the enzymes
418 involved may therefore be good chemotherapeutic targets (Martínez *et al*., 2002; López
419 and Segura Latorre, 2008). As cells must be compartmentalized in unicellular
420 organisms, in the present study we mainly focused on Ca^{2+} regulation and acidic stores
421 to identify potential targets involved in bioenergetics, which can be modulated in
422 infected fish. The *P. dicentrarchi* H^+-PPase is located in the membranes of endocytic
423 vacuoles and alveolar sacs (both acidic compartments), as demonstrated by acridine
424 orange and Lysotracker Red staining and which is consistent with our previous
425 observations (Mallo et al., 2015; 2016a). H^+-PPase promotes acidification of these
426 compartments and could therefore interfere in the adaptive response of the ciliate to
427 maintaining osmoregulation and pH homeostasis, by performing similar functions as in
428 acidocalcisomes (Docampo *et al*, 2005; Pan *et al*., 2011; Mallo *et al.,* 2015). In the
429 present study, we also observed a wide variation in the pH of alveolar sacs and
430 endocytic vacuoles, which probably reflects the role that these cellular compartments
431 play in regulating intracellular pH, as occurs with acidocalcisomes in other protozoan
432 parasites (Docampo et al., 2013).

433 Some electron-dense deposits were observed in the cytosolic region and alveolar
434 sacs, where the H^+-PPase enzyme is located (Mallo *et al.,* 2015). The same distribution
435 pattern was observed for Ca^{2+}, with the Fluo-4 NW probe. These electron-dense
436 deposits are also characteristic of acidocalcisomes (Miranda et al., 2000, 2004, 2008;

Soares-Medeiros et al., 2005), which share some of their features with alveolar sacs of *P.dicentrarchi,* such as their acidic origin, their function as Ca^{2+} stores and possession of some of the enzymes involved in acidification (e.g. H^+-PPase). Acridine orange staining and enzyme immunolocalization showed that some alveolar sacs are located under the cilia, indicating that they are involved in ciliary movement and/or bioenergetics (Plattner and Klauke, 2001).

The presence of enzymes and exchangers that cooperate in pH maintenance in acidocalcisomes, such as H^+-PPase, H^+- ATPase, Na^+/H^+ and Ca^{2+}/H^+ exchangers, may interfere in release of Ca^{2+} from internal stores via modification of pH due to H^+ translocation and associated activity (Marchesini *et al*., 2000; Vercesi *et al*., 2000; Saliba *et al*., 2003; Moriyama *et al*., 2003).

Movement of H^+ between intracellular membranes can be divided into two different categories: those coupled to ATP production and those with a purpose other than energy production, such as acidification (Rudnick, 1987). Sequencing of the complete genome of some ciliate species has led to identification of H^+-ATPase in organelle membranes of *Paramecium* (Plattner, 2010), and the main function of this ATPase seems to be osmoregulation and pH homeostasis (Van der Heyden and Docampo, 2002; Wassmer *et al*., 2005), i.e. similar functions to those of H^+-PPase. H^+-ATPase activity has been measured in different organisms by use of acridine orange as an indicator of acidification. Unlike in other organisms, addition of ATP inhibits H^+ translocation in permeabilized specimens of *P. dicentrarchi*, resulting in alkalinization of vacuoles, as occurs with addition of NH_4Cl, used as a control for alkalinization at the end of all experiments as it eliminates H^+ from acidic compartments (Docampo *et al*., 1995; Rodrigues *et al*., 1999a; Ruíz *et al*., 2001). H^+-ATPase has been described as a Ca^{2+} insensitive enzyme, unlike H^+-PPase (Rea *et al*., 1992), and total blockage of H^+

462 pumping activity by Ca^{2+} may indicate that this activity does not take place through the
463 H^+-ATPase route, as occurs in *P. dicentrarchi*. This phenomenon has also been
464 observed in the trypanosomatid *Herpetomonas* (Soares Medeiros *et al*., 2005), in which
465 ATP did not promote H^+ uptake. In *Streptococcus faecalis*, PPase is inhibited by ATP,
466 which competes with PPi for chelation of Mg^{2+} ions (Lahti and Lonnberg, 1985), in
467 which Mg_2PPi is the main substrate. It is also possible that H^+-PPase activity is inhibited
468 by excess Pi formed as a product of ATP metabolism (ADP + Pi), induced by excess
469 ATP. Another possible explanation for the inability of ATP
470 to induce H^+ translocation may be related directly to the DIG used in permeabilization
471 of cells that could generate an alteration in cholesterol levels of intracellular
472 compartments, causing incapability to measure ATP-driven H^+ transport in DIG-
473 permeabilized cells (Rodrigues et al., 2001). Inhibition of H^+-PPase by Ca^{2+} has been
474 described through formation of the CaPPi complex, which competes with the enzyme
475 substrate or the Ca^{2+} ion, mimicking Mg^{2+} and inhibiting enzymatic activity (Maeshima,
476 1991; Rea et al., 1992). Moreover, H^+ release as a consequence of the addition of Ca^{2+}
477 in *P. dicentrarchi* suggests that an exchanger of Ca^{2+}/H^+ takes place in the membranes
478 of acidic compartments as occurs in the trypanosomatid *Herpetomonas* (Soares
479 Medeiros *et al.*, 2005).

480 In *P. dicentrarchi*, NaCl enhances H^+ release, thus leading to the alkalinization
481 of acidic compartments. Because H^+ translocation in the ciliate mainly occurs via H^+-
482 PPase activity, NaCl may act as an inhibitor of this enzyme. Although this is not
483 common in H^+-PPases (Fukuda *et al*., 2004), a subtype of H^+-PPase that is inhibited by
484 Na^+ has recently been characterized; however, this phenomenon has been only observed
485 in prokaryotes and is believed to be an evolutionary remnant (Luoto *et al*., 2013; 2015).
486 Similar observations have been made in the trypanosomatid parasite *Herpetomonas*, in

487 which NaCl-mediated inhibition of PPi-dependent H^+ uptake has been detected (Soares
488 Medeiros *et al*., 2005), and also in *Leishmania donovani*, in which NaCl does not
489 stimulate H^+ translocation (Sen *et al*., 2009). The NaCl probably reverses acidification,
490 as occurs in the parasite *T. gondii*, because of the presence of a Na^+/H^+ exchanger. The
491 effect of Na^+ was observed independently of the addition of PPi, indicating that the
492 effect on acidification is not related to that promoted by PPi. NaCl was added during
493 preparation of the sample in KCl buffer, indicating that the observed effect was not due
494 to changes in osmolarity (Rohloff *et al.,* 2011).

495 As ATP and Ca^{2+} induced alkalinization of compartments in *P. dicentrarchi*,
496 their effect on H^+-PPase expression was evaluated, and it was found that they inhibited
497 both protein and gene expression. ATP and Ca^{2+} probably inhibit expression and
498 activity of the H^+-PPase in the ciliate. If the Ca^{2+}-ATPase pump is present in the ciliate,
499 any excess ATP and Ca^{2+} could interact with Ca^{2+} and Na^+ exchangers, so that H^+-PPase
500 activity would not be required for H^+ translocation.

501 Regulation of Ca^{2+} has been investigated in depth in *Paramecium* and has been
502 implicated in multiple functions and cell survival. Maintenance of acidification is
503 responsible for Ca^{2+} retention in acidic compartments such as acidocalcisomes. The
504 contractile vacuole of *Paramecium* and *Dictyostelium discoideum* also appears to be
505 important in regulating the internal Ca^{2+} concentration (Stock *et al*., 2002, Pittman *et*
506 *al*., 2011; Martínez-Higuera *et al*., 2013). In *Trypanosoma,* the Ca^{2+}-ATPase, H^+-
507 ATPase and H^+-PPase enzymes are suggested as being responsible for Ca^{2+}
508 accumulation in acidocalcisomes (Docampo and Moreno, 2001; De Souza *et al.,* 2002).
509 As salinity may modulate Ca^{2+} channels in *P. dicentrarchi* and the H^+-PPase enzyme
510 interferes with acidification of the Ca^{2+} compartment, different concentrations of NaCl
511 and PPi were added to study how these compounds interfere in intracellular Ca^{2+}

512 regulation. PPi downregulates Ca^{2+} levels, which could be explained as upregulation of
513 H^+-PPase activity. Addition of PPi, with the consequent generation of excess H^+ inside
514 the vacuole, may activate Na^+/H^+ exchange, thus eliminating Ca^{+2} from the stores via
515 Ca^{2+}/H^+ exchange and producing an increase in cytosolic Ca^{+2}, as described in another
516 organisms (Bonansea *et al*., 2012). In the plant pathogen *Phytoptora infestans*, addition
517 of PPi stimulates Ca^{+2} transport (Okorokov *et al*, 1978). Saline conditions lead to
518 alkalinization of the vacuoles, and NaCl may therefore act at the Na^+/H^+ exchange level,
519 coupled to Ca^{2+}/H^+ transport, to downregulate Ca^{+2} levels at low concentrations of
520 NaCl.

521 In conclusion, our findings confirm the existence in *P. dicentrarchi* of Ca^{2+}
522 acidic store organelles, which appear to have similar functions to the acidocalcisomes
523 described in Apicomplexan parasites (i.e. modulation of Ca^{2+} levels and osmolarity).
524 Regulation of the intracellular pH of these compartments may represent a new target for
525 development of chemotherapeutic treatments against scuticociliatosis (Mallo et al.,
526 2016b). This has already been done in other parasites e.g. disruption of pH regulation in
527 the parasite acidocalcisome has been used in developing antimalarial agents (Docampo
528 and Moreno, 2008; Van Schalkwyk, *et al.*, 2010).

529

530 Acknowledgements

531 This study was financially supported by grants AGL2014-57125-R and
532 AGL2014-53190-REDC from the Ministerio de Economía y Competitividad (Spain), by
533 grant GPC2014/069 from the Xunta de Galicia (Spain), and by PARAFISHCONTROL
534 project. This project has received funding from the *European Union's Horizon 2020*
535 *research and innovation programme* under grant agreement No. 634429. This
536 publication reflects the views only of the authors, and the European Commission cannot

be held responsible for any use which may be made of the information contained therein.

References

Baltscheffsky M, Schultz A, Baltscheffsky H., 1999. H^+-PPases a tightly membrane-bound family. FEBS Lett 457, 527-533.

BonanseaS, Usorach M, Gesumaría MC, Santander V, Giménez AM, Bollo M, Machado EE., 2012. Stress response to high osmolarity in *Trypanosoma cruzi* epimastigotes. Arch Biochem Biophys 527, 6-15.

Bradford MM., 1976. A rapid and sensitive method for the quantitation of microgram quantities of protein utilizing the principle of protein-dye binding. Anal Biochem 72, 248-254.

Budiño B, Lamas J, Pata MP, Arranz JA, Sanmartín ML, Leiro J., 2011. Intraspecific variability in several isolates of *Philasterides dicentrarchi* (syn. *Miamiensis avidus*), a scuticociliate parasite of farmed turbot. Vet Parasitol 175, 260-272.

Bustin SA, Benes V, Garson JA, Hellemans J, Huggett J, Kubista M, Mueller R, Nolan T, Pfaffl MW, Shipley GL, Vandesompele J, Wittwer CT., 2009. The MIQE guidelines: minimum information for publication of quantitative real-time PCR experiments. Clin Chem 55, 611-622.

De Souza W, Attias M, Rodrigues JC., 2009. Particularities of mitochondrial structure in parasitic protists (Apicomplexa and Kinetoplastida). Int J Biochem Cell Biol 41, 2069-2080.

Docampo R, Scott DA, Vercesi AE, Moreno SNJ., 1995. Intracellular Ca^{2+} storage in acidocalcisomes of *Trypanosoma cruzi*. Biochem J 310, 1005-1012.

562 Docampo R, Moreno SN., 2001. The acidocalcisome. Mol Biochem Parasitol 114, 151-
563 159.
564 Docampo R, Moreno SN., 2011. Acidocalcisomes. Cell Calcium 50, 113–119.
565 Docampo R, de Souza W, Miranda K, Rohloff P, Moreno SN., 2005. Acidocalcisomes -
566 conserved from bacteria to man. Nat Rev Microbiol 3, 251-261.
567 Docampo R, Moreno SN., 2008. The acidocalcisome as a target for chemotherapeutic
568 agents in protozoan parasites. Curr Pharm Des 14, 882-888.
569 Docampo R, Jiménez V, Lander N, Li ZH, Niyogi S., 2013. New insights into roles of
570 acidocalcisomes and contractile vacuole complex in osmoregulation in protists.
571 Int Rev Cell Mol Biol 305, 69-113.
572 Dragesco A, Dragesco J, Coste F, Gasc C, Romestand B, Raymond J, Bouix G., 1995.
573 *Philasterides dicentrarchi*, n. sp., (Ciliophora, Scuticociliatida), a histophagous
574 opportunistic parasite of *Dicentrarchus labrax* (Linnaeus, 1758), a reared marine
575 fish. Eur J Protistol 31, 327-340.
612 Friedrich O, Reiling SJ, Wunderlich J, Rohrbach P., 2014. Assessment of *Plasmodium*
613 *falciparum* PfMDR1 transport rates using Fluo-4. J Cell Mol Med 18, 1851-
614 1862.
615 Fukuda A, Chiba K, Maeda M, Nakamura A, Maeshima M, Tanaka Y., 2004. Effect of
616 salt and osmotic stresses on the expression of gene for the vacuolar H^+-
617 pyrophosphatase, H^+-ATPase subunit A, and Na^+/H^+ antiporter from barley. J
618 Exp Bot 55, 585-594.
619 Garcia CR, Ann SE, Tavares ES, Dluzewski AR, Mason WT, Paiva FB., 1998. Acidic
620 calcium pools in intraerythrocytic malaria parasites. Eur J Cell Biol 76, 133-138.
621 Gaxiola RA, Palmgren MG, Schumacher K., 2007. Plant proton pumps. FEBS Lett 581,
622 2204-2214.

623 Hannaert V, Saavedra E, Duffieux F, Szikora JP, Rigden DJ, Michels PAM, Opperdoes
624 FR., 2003. Plant-like traits associated with metabolism of *Trypanosoma*
625 parasites. Proc Natl Acad Sci USA 100, 1067-1071.
626 Heinonen JK., 2003. Biological Role of inorganic pyrophosphate. Springer Science +
627 Bussines Media LLC, Finland.
628 Hill JE, Scott DA, Luo S, Docampo R., 2000. Cloning and functional expression of a
629 gene encoding a vacuolar-type proton-translocating pyrophosphatase from
630 *Trypanosoma cruzi*. Biochem J 351, 281-288.
631 Iglesias R, Paramá A, Álvarez MF, Leiro J, Fernández J, Sanmartín ML., 2001.
632 *Philasterides dicentrarchi* (Ciliophora, Scuticocilatida) as the causative agent of
633 scuticociliatosis in farmed turbot *Scophthalmus maximus* in Galicia (NW Spain).
634 Dis Aquat Organ 46, 47–55.
635 Iglesias R, Paramá A, Álvarez MF, Leiro J, Aja C, Sanmartín ML., 2003. *In vitro*
636 growth requirements for the fish pathogen *Philasterides dicentrarchi*
637 (Ciliophora, Scuticociliatida). Vet Parasitol 111, 19-30.
638 Ito H, Fukuda Y, Murata K, Kimura A., 1983. Transformation of intact yeast cells
639 treated with alkali cations. J Bacteriol 153, 163-168.
640 Kaneshiro ES, Dunham PB, Holz GG., 1969. Osmorregulation in a marine ciliate,
641 *Miamiensis avidus*. I. Regulation of inorganic ions and water. Biol Bull 136, 63-
642 75.
643 Kim K, Son M, Peterson JB, Nelson DL, 2002. $Ca^{(2+)}$-binding proteins of cilia and
644 infraciliary lattice of *Paramecium tetraurelia*: their phosphorylation by purified
645 endogenous $Ca^{(2+)}$ dependent protein kinases. J Cell Sci 115, 1973-1984.
646 Kissmehl R, Krüger TP, Treptau T, Froissard, M, Plattner H., 2006.
647 Multigene family encoding 3',5'-cyclic-GMP

dependent protein kinases in *Paramecium tetraurelia* cells. Eukaryot Cell 5, 77-91.

Lahti R, Lónnberg H., 1985. Comparative kinetic studies on the two interconvertible forms of *Streptococcus faecalis* inorganic pyrophosphatase. Biochem J 231, 485-488.

Leiro J, Piazzón MC, Budiño B, Sanmartín ML, Lamas J., 2008. Complement-mediated killing of *Philasterides dicentrarchi* (Ciliophora) by turbot serum: relative importance of alternative and classical pathways. Par Immunol 30, 535-543.

Lemercier G, Dutoya S, Luo S, Ruiz FA, Rodrigues CO, Baltz T, Docampo R, Bakalara N., 2002. A vacuolar-type H^+ pyrophosphatase governs maintenance of functional acidocalcisomes and growth of the insect and mammalian forms of *Trypanosoma brucei*. J Biol Chem 277, 37369-37376.

Li FJ, He CY., 2014. Acidocalcisome is required for autophagy in *Trypanosoma brucei*. Autophagy 10, 1978-1988.

Livak KJ, Schmittgen TD., 2001. Analysis of relative gene expression data using real-time quantitative PCR and the 2- Delta Delta Ct method. Methods 25, 402–408.

López ML, Segura-Latorrem C., 2008. The new permeability pathways and cytosolic pH: Targets for antimalarial agents on *Plasmodium falciparum*. Act Biol Colomb 13, 3-22.

López-López O, Fuciños P, Pastrana L, Rúa ML, Cerdán ME, González-Siso MI., 2010. Heterologous expression of an esterase from *Thermus thermophilus* HB27 in *Saccharomyces cerevisiae*. J Biotechnol 145, 226-232.

Luo S, Vieira M, Graves J, Zhong L, Moreno SN., 2001. A plasma membrane-type $Ca(^{2+})$-ATPase co-localizes with a vacuolar $H(^{+})$-pyrophosphatase to acidocalcisomes of *Toxoplasma gondii*. EMBO J 20, 55-64.

673 Luoto HH, Baykov AA, Lahti R, Malinen AM., 2013. Membrane-integral
674 pyrophosphatase subfamily capable of translocating both Na^+ and H^+. Proc Natl
675 Acad Sci USA 110, 1255-1260.
676 Luoto HH, Nordbo E, Malinen AM, Baykov AA, Lahti R., 2015. Evolutionarily
677 divergent, Na^+-regulated H^+-transporting membrane-bound pyrophosphatases.
678 Biochem. J 467, 281-291.
679 Lynn DH, Corliss JO., 1991. Phylum Ciliophora. In *Microscopic Anatomy of*
680 *Invertebrates*, pp. 333-467. Harrison, F.W., Corliss, J.O. (eds.), Alan R. Liss,
681 New York Inc.
682 Maeshima M., 1991. $H(^+)$-translocating inorganic pyrophosphatase of plant vacuoles.
683 Inhibition by $Ca^{2+,}$ stabilization by Mg^{2+} and immunological comparison with
684 other inorganic pyrophosphatases. Eur J Biochem 196, 11-17.
685 Mallo, N., Lamas, J., Piazzon, C., Leiro, J.M., 2015. Presence of a plant-like proton-
686 translocating pyrophosphatase in a scuticociliate parasite and its role as a
687 possible drug target. Parasitology 142, 449-462.
688 Mallo N, Lamas J, De Felipe AP, De Castro ME, Sueiro R, Leiro JM., 2016a. Presence
689 of an isoform of H^+-pyrophosphatase located in the alveolar sacs of a
690 scuticociliate parasite of turbot: physiological consequences. Parasitology 143,
691 576-587.
692 Mallo N, Lamas J, DeFelipe AP, Sueiro RA, Fontenla F, Leiro J., 2016b. Enzymes
693 involved in pyrophosphate and calcium metabolism as targets for anti-
694 scuticociliate chemotherapy. J Eukaryot Microbiol (In press).
695 Marchesini N, Luo S, Rodrigues CO, Moreno SNJ, Docampo R., 2000.
696 Acidocalcisomes and vacuolar H^+-pyrophosphatase in malaria parasites.
697 Biochem J 347, 243-253.

698 Maroulis SL, Schofield PJ, Edwards MR., 2003. Osmoregulation in the parasitic
699 protozoan *Tritrichomonas foetus*. Appl Environ Microbiol 69, 4527-4533.
700 Martínez R, Wang Y, Benaim G, Benchimol M, de Souza W, Scott DA, Docampo, R.,
701 2002. A proton pumping pyrophosphatase in the Golgi apparatus and plasma
702 membrane vesicles of *Trypanosoma cruzi*. Mol Biochem Parasitol 120, 205-213.
703 Martínez-Higuera A, Salas-Casas A, Calixto-Gálvez M, Chávez-Munguía B, Pérez-
704 Ishiwara DG, Ximénez C, Rodríguez MA., 2013. Identification of calcium-
705 transporting ATPases of *Entamoeba histolytica* and cellular localization of the
706 putative SERCA. Exp Parasitol 135: 79-86.
707 Miranda K, Benchimol M, Docampo R, de Souza W., 2000. The fine structure of
708 acidocalcisomes in *Trypanosoma cruzi*. Parasitol Res 86, 373-384.
709 Miranda K, Docampo R, Grillo O, Franzen A, Attias M, Vercesi A, Plattner H,
710 Hentschel J, de Souza W., 2004. Dynamics of polymorphism of
711 acidocalcisomes in *Leishmania* parasites. Histochem. Cell Biol 1121, 407-
712 418.
713 Miranda K, de Souza W, Plattner H, Hentschel J, Kawazoe U, Fang J, Moreno SN.,
714 2008. Acidocalcisomes in Apicomplexan parasites. Exp Parasitol 118, 2-9.
715 Moreno SNJ, Docampo R., 2009. The role of acidocalcisomes in parasitic protists.
716 J Eukaryot Microbiol 56, 208-213.
717 Moriyama Y, Hayashi M, Yatsushiro S, Yamamoto A., 2003. Vacuolar proton pumps
718 in malaria parasite cells. J Bioenerg Biomembr 35, 367-375.
719 Nisbet B., 1984. Nutrition feeding strategies in protozoa. Croom Helm, Australia Pty
720 Ltd.

721 Okorokov LA, Sysuev VA, Kulaev IS., 1978. Pyrophosphate-stimulated uptake of
722 calcium into the germlings of *Phytophthora infestans.* Eur J Biochem 83, 507-
723 511.
724 Pan YJ, Lee CH, Hsu SH, Huang YT, Lee CH, Liu TH, Chen YW, Lin SM, Pan RL.,
725 2011. The transmembrane domain 6 of vacuolar H($^{+}$)-pyrophosphatase mediates
726 protein targeting and proton transport. Biochim Biophys Acta 1807, 59-67.
727 Paramá A, Iglesias R, Álvarez MF, Leiro J, Aja C, Sanmartín ML., 2003. *Philasterides*
728 *dicentrarchi* (Ciliophora, Scuticociliatida): experimental infection and possible
729 routes of entry in farmed turbot (*Scophthalmus maximus*). Aquaculture 217, 73–
730 80.
731 Paramá A, Arranz JA, Álvarez MF, Sanmartín ML, Leiro J., 2006. Ultrastructure and
732 phylogeny of *Philasterides dicentrarchi* (Ciliophora, Scuticociliatia) from
733 farmed turbot in NW. Parasitology 132, 555-564.
734 Paredes RM, Etzler JC, Watts LT, Zheng W, Lechleiter JD., 2008. Chemical calcium
735 indicators. Methods 46, 143–151.
736 Piazzón C, Lamas J, Castro R, Budiño B, Cabaleiro S, Sanmartín ML, Leiro J., 2008.
737 Antigenic and cross-protection studies on two turbot scuticociliate isolates. Fish
738 Shellfish Immunol. 25, 417-424.
739 Pittman JK., 2011. Vacuolar Ca^{2+} uptake. Cell Calcium 50,139-146.
740 Plattner H., 2010. Membrane trafficking in protozoa SNARE proteins, H+-ATPase,
741 actin, and other key players in ciliates. Int Rev Cell Mol Biol 280, 79-184.
742 Plattner, H., 2014. Calcium signalling in the ciliated protozoan model, *Paramecium*:
743 Strict signal localization by epigenetically controlled positioning of different
744 Ca^{2+}-channels. Cell Calcium 57, 203-213.

745 Plattner H., 2015. Molecular aspects of calcium signalling at the crossroads of
746 unikont and bikont eukaryote evolution – The ciliated protozoan *Paramecium* in
747 focus. Cell Calcium 57, 174–185.
748 Plattner H, Klauke N., 2001. Calcium in ciliated protozoa: sources, regulation, and
749 calcium-regulated cell functions. Int Rev Cytol 201, 115-208.
750 Rea PA, Kim Y, Sarafian V, Poole RJ, Davies JM, Sanders D., 1992. Vacuolar H^+-
751 translocating pyrophosphatases: a new category of ion translocase. Trends
752 Biochem Sci 17, 348-353.
753 Rohloff P, Docampo R., 2006. Ammonium production during hypo-osmotic stress
754 leads to alkalinization of acidocalcisomes and cytosolic acidification in
755 *Trypanosoma cruzi*. Mol Biochem Parasitol 150, 249–255.
756 Rohloff P, Docampo RA., 2008. Contractile vacuole complex is involved in
757 osmoregulation in *Trypanosoma cruzi*. Exp Parasitol 118: 17-24.
758 Rohloff P, Miranda K, Rodrigues JC, Fang J, Galizzi M, Plattner H, Hentschel J,
759 Moreno SN., 2011. Calcium uptake and proton transport by acidocalcisomes of
760 *Toxoplasma gondii*. PLoS One 6, e18390.
761 Rodrigues CO, Scott DA, Docampo R., 1999a. Presence of a vacuolar H^+-
762 pyrophosphatase in promastigotes of *Leishmania donovani* and its localization to
763 a different compartment from the vacuolar H^+-ATPase. Biochem J 340, 759-766.
764 Rodrigues CO, Scott DA, Docampo R., 1999b. Characterization of a vacuolar
765 pyrophosphatase in *Trypanosoma brucei* and its localization to acidocalcisomes.
766 Mol Cell Biol 19, 7712-7723.
767 Rodrigues CO, Scott DA, de Souza W, Benchimol M, Urbina JA, Oldfield E, Moreno
768 SN., 2000. Vacuolar proton pyrophosphatase activity (PPi) in *Toxoplasma*
769 *gondii* as possible chemotherapeutic target. Biochem J 349, 737-745.

Rodrigues CO, Catisti R, Uyemura SA, Vercesi AE, Lira R, Rodriguez C, Urbina JA, Docampo R., 2001. The sterol composition of *Trypanosoma cruzi* changes after growth in different culture media and results in different sensitivity to digitonin-permeabilization. J Eukaryot Microbiol 48, 588-594.

Rodrigues CO, Ruiz FA, Rohloff P, Scott DA, Moreno SNJ., 2002. Characterization of isolated acidocalcisomes from *Toxoplasma gondii* tachyzoites reveals a novel pool of hydrolyzable polyphosphate. J Biol Chem 277, 48650–48656.

Rudnick G., 1987. ATP_Driven H^+ Pumping into Intracellular Organelles. Ann Rev Physiol 48, 403-413.

Ruíz FA, Marchesini N, Seufferheld M, Govindjee, Docampo R., 2001. The polyphosphate bodies of *Chlamydomonas reinhardtii* possess a proton-pumping pyrophosphatase and are similar to acidocalcisomes. J Biol Chem 276, 46196–46203.

Sahoo N, Labruyère E, Bhattacharya S, Sen P, Guillén N, Bhattacharya A., 2004. Calcium binding protein of the protozoan parasite *Entamoeba histolytica* interacts with actin and is involved in cytoskeleton dynamics. J Cell Sci 117, 3625-3634.

Saliba KJ, Allen RJ, Zissis S, Bray PG, Ward SA, Kirk K., 2003. Acidification of the malaria parasite's digestive vacuole by a H^+-ATPase and a H^+-pyrophosphatase. J Biol Chem 278, 5605-5612.

Sen SS, Bhuyan NR, Bera T., 2009. Characterization of plasma membrane bound inorganic pyrophosphatase from *Leishmania donovani* promastigotes and amastigotes. Afr Health Sci 9, 212-217.

793 Soares Medeiros LCA, Moraes Moreira BL, Miranda K, de Souza W, Plattner H,
794 Hentschel J, Barrabin H., 2005. A proton pumping pyrophosphatase in
795 acidocalcisomes of *Herpetomonas* sp. Mol Biochem Parasitol 140, 175–182.
796 Stelly N, Halpern S, Nicolas G, Fragu P, Adoutte A., 1995. Direct visualization of a
797 vast cortical calcium compartment in *Paramecium* by secondary ion mass
798 spectrometry (SIMS) microscopy: possible involvement in exocytosis. J Cell Sci
799 108, 1895-1909.
800 Stock C, Grønlien HK, Allen RD., 2002. The ionic composition of the contractile
801 vacuole fluid of *Paramecium* mirrors ion transport across the plasma membrane.
802 Eur J Cell Biol 81, 505-515.
803 Takahashi A, Camacho P, Lechleiter JD, Herman B., 1999. Measurement of
804 intracellular calcium. Physiol Rev 79, 1089-1125.
805 Van Der Heyden N, Docampo R., 2002. Proton and sodium pumps regulate the plasma
806 membrane potential of different stages of *Trypanosoma cruzi*. Mol Biochem
807 Parasitol 120, 127–139.
808 Van Schalkwyk DA, Chan XW, Misiano P, Gagliardi S, Farina C, Saliba KJ., 2010.
809 Inhibition of *Plasmodium falciparum* pH regulation by small molecule indole
810 derivatives results in rapid parasite death. Biochem Pharmacol 79, 1291-1299.
811 Vercesi AE, Rodrigues CO, Catisti R, Docampo R., 2000. Presence of a Na(+)/H(+)
812 exchanger in acidocalcisomes of *Leishmania donovani* and their alkalization by
813 anti-leishmanial drugs. FEBS Lett 473, 203-206.
814 Wang Y, Miao M, Zhang Q, Gao S, Song W, Al-Rasheid KAS, Warren A, Ma H.,
815 2008. Three marine interstitial scuticociliates, *Schizocalyptra similis* sp. n., *S.*
816 *sinica* sp. n. and *Hippocomos salinus* Small and Lynn, 1985 (Ciliophora:

817 Scuticociliatida), isolated from Chinese coastal waters. Acta Protozool 47: 377–
818 387.
819 Wassmer T, Sehring IM, Kissnehl R, Plattner H., 2009. The V-ATPase in *Paramecium*:
820 functional specialization by multiple isoforms. Pflugers Arch –Eur J Physiol
821 457, 599-607.
822 Wassmer T, Froissard M, Plattner H, Kissmehl R, Cohen J., 2005. The vacuolar proton-
823 ATPase plays a major role in several membrane-bounded organelles in
824 *Paramecium*. J Cell Sci 118, 2813-2825.
825 Zhen RG, Kim EJ, Rea P., 1997. The molecular and biochemical basis of
826 pyrophosphatase energized proton translocation at the vacuolar membrane. Adv
827 Bot Res 25, 297-337.

Figures

Figure 1: Distribution of calcium and acidic compartments in *P. dicentrarchi*. A1 and A2) Intracellular acidic compartments stained with acridine orange and Lysotracker Red 99-DND. In A1, intense fluorescent staining of the alveolar sacs with the dyes Lysotracker and acridine orange is observed (arrowheads). The frame a) shows a *P. dicentrarchi* trophozoite dyed only with acridine orange showing differences in intensity of fluorescence and colour (red/orange/yellow/green) in the endocytic vacuoles (arrows). The frame b) shows a trophozoite treated with the pyrophosphate analogous and regulator of the Ca^{2+} metabolism, pamidronate (PAM) at 0.1 mM where a green fluorescent labeling of the vesicles stained with acridine orange is observed indicating its alkali state (arrows). In A2, staining of alveolar sacs with Lysotracker/acridine orange is consistent with the ciliary pattern in kinetia (arrowheads). B) The Fluo 4-NW Calcium probe revealed the calcium stores distributed in alveolar sacs (arrowheads) and endocytic internal vacuoles (arrows). C) Immunolocalization of H^+-PPase with recombinant anti-H^+-PPase labelling of alveolar sacs (arrowheads) and some internal vacuole membranes (arrows) of the ciliate. Bar scale = 10 μm.

Figure 2: Transmission electron microscope (TEM) photomicrograph of a *P. dicentrarchi* trophozoite. A) Panoramic view of an ultrathin section showing alveolar sacs beneath the plasma membrane and containing a spherical electron-dense body (arrows). The presence of electron-dense bodies was also observed in the interior of the cytoplasmic vacuoles (arrowheads). B) Enlargement of the surface of a trophozoite with an electron dense body (arrow) in the interior of

alveolar sacs (as). Mitochondria (m) are also observed in close contact with the inner membrane of the alveolar sacs. N = nucleus.

Figure 3: Effect of ATP and Ca^{2+} on H^+ translocating activity. H^+ translocation activity in the presence and absence of PPi (A), ATP (B), PPi and ATP (C) and Ca^{2+} or pamidronate –PAM-(D). The concentrations used (indicated) were achieved by addition of stock solutions prepared in assay buffer. The results show the mean values ± standard error (n=5) of the variation (Δ) in fluorescence. Asterisks indicate statistically significant differences ($^{*}P < 0.05$; $^{**}P < 0.01$).

Figure 4: Effect of ATP and Ca^{2+} on H^+-PPase protein and gene expression. A) Western blot showing the recognition pattern of an H^+-PPase (rH^+-Ppase) recombinant polyclonal antibody against ciliate vesicle enriched samples in non-reducing conditions (without DTT). Ciliates were incubated with 1mM ATP (lane 2) or with 0.8 mM $CaCl_2$ (lane 3) for 6h. Lane 1 corresponds to the control. Mw: molecular weight marker proteins. B) The band intensity of Western blot assay (in arbitrary units) was measured with Total Lab, and statistical comparisons were made relative to the control. C) H^+-PPase gene expression levels in ciliates treated for 24 hours with 1 mM ATP and 0.8 mM $CaCl_2$. Expression was analyzed by RT-qPCR. The *P. dicentrarchi* β-tubulin was used as reference gene. As shown in both cases, calcium and ATP induced a decrease in gene expression. The bars in the graphs show the results as mean ± standard error (n= 5). Asterisks indicate the statistically significance * $P < 0.05$, ** $P < 0.01$

Figure 5: A) Effect of NaCl and KCl (100 mM) on the H^+ translocating activity induced by PPi. The results show the mean values ± standard error (n=5) of the variation (Δ) in fluorescence. B) Effect of salinity and PPi on calcium levels. Ciliates were

877 incubated for 24 hours in saline solutions of 4 and 8 ‰. 1 mM PPi was then
878 added and the ciliates were incubated for a further1 h. The calcium probe (Fluo-
879 4 NW) was then added and after 1 hour, fluorescence (Ex: 494 nm, Em: 516 nm)
880 was measured, in arbitrary units (AU). Bars represent the mean (± standard
881 error; n= 5) and letters indicate statistically significance between groups ($^{*}P<$
882 0.05, $^{**}P<$ 0.01).

Figure
Click here to download high resolution image

Figure 1

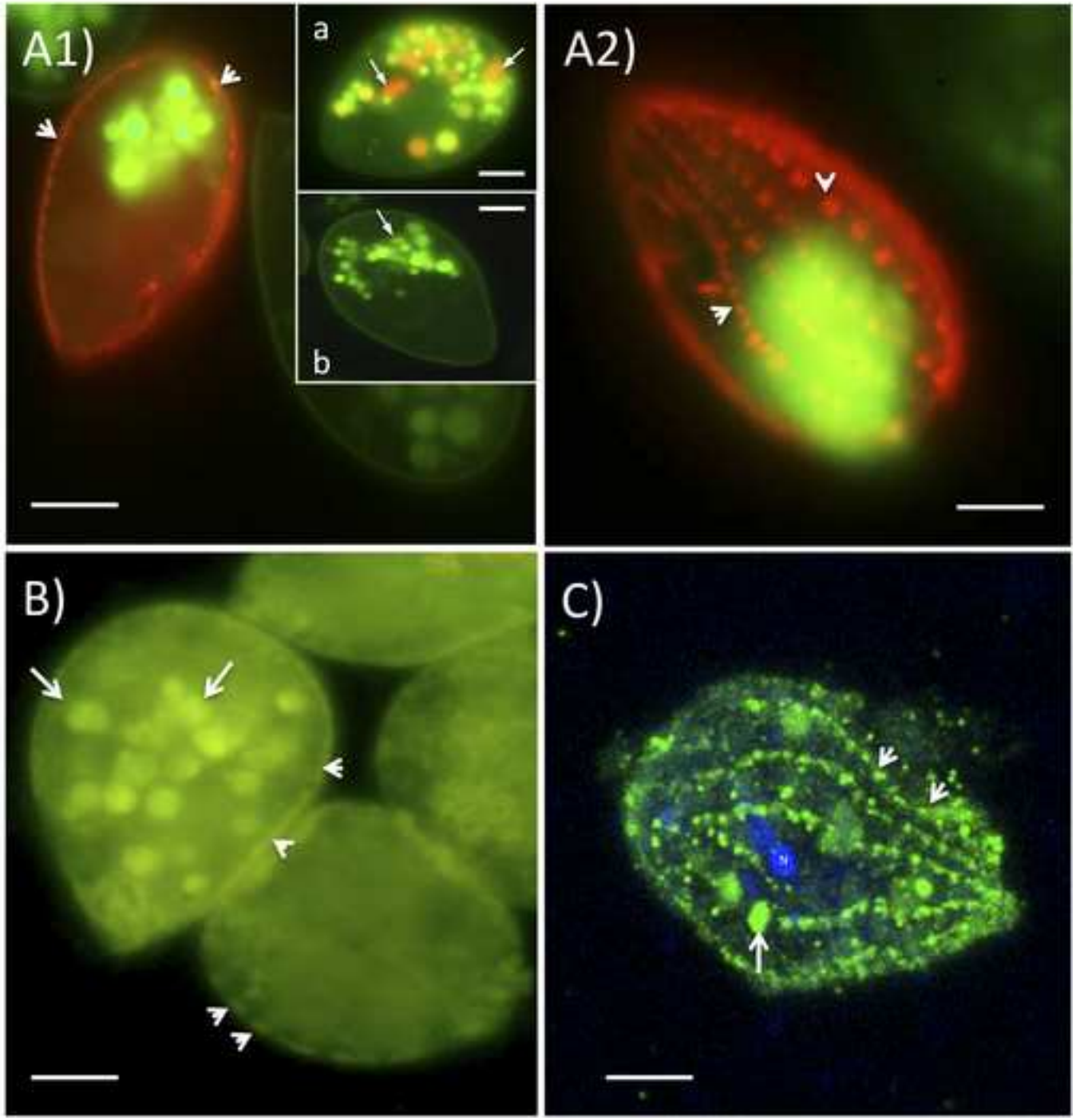

Figure2
Click here to download high resolution image

Figure 2

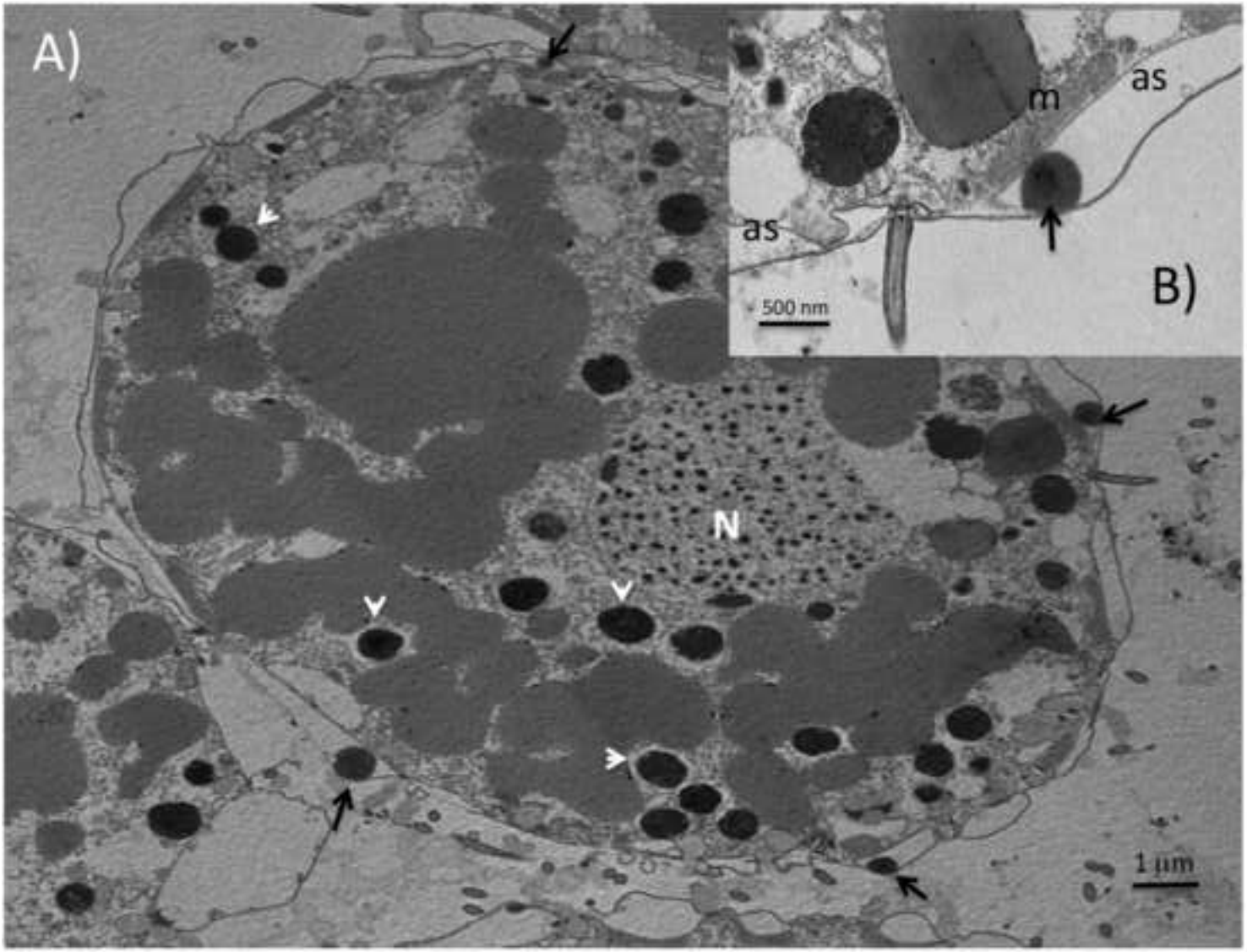

Figure3

Click here to download high resolution image

Figure 3

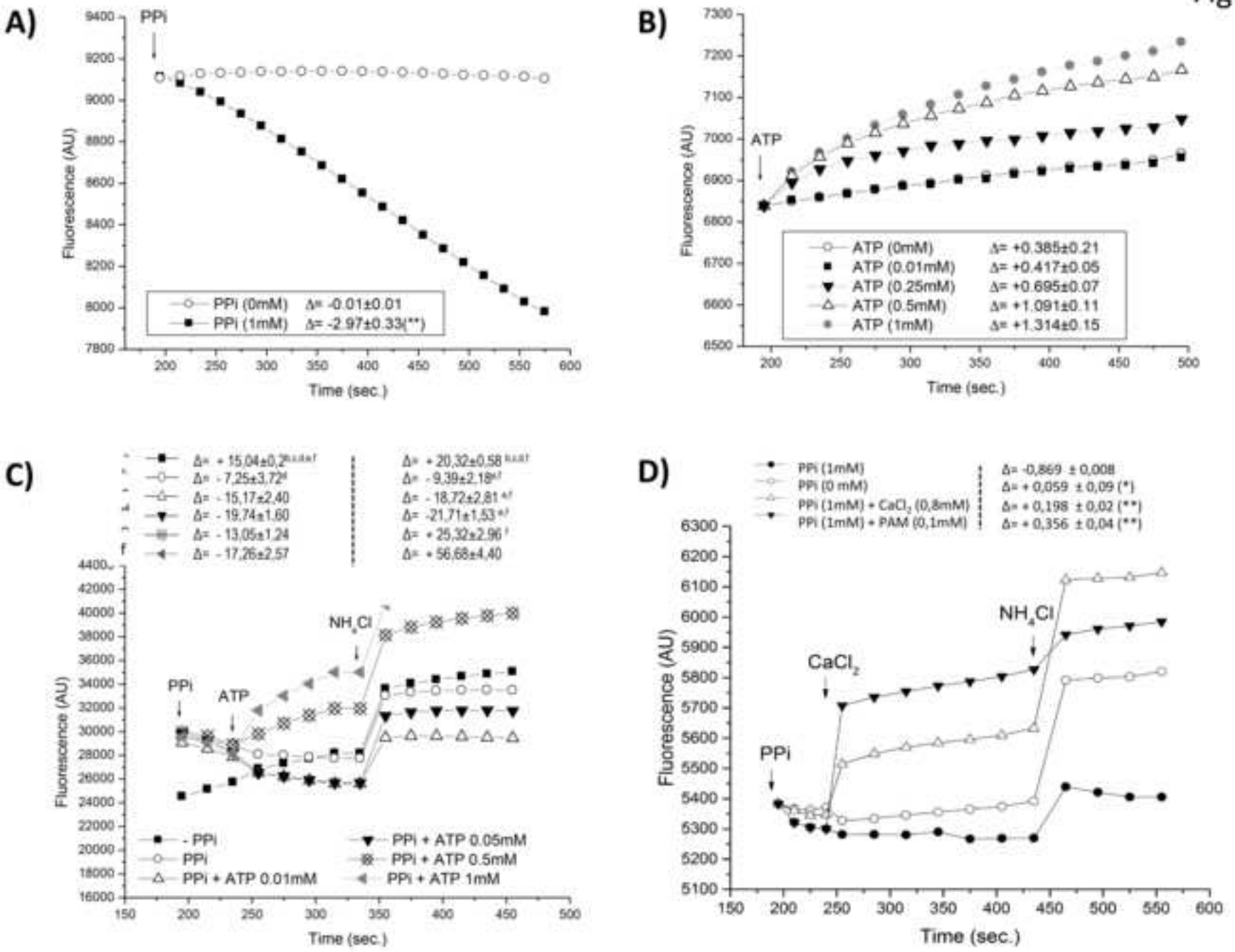

Figure4

Click here to download high resolution image

FIGURE 4

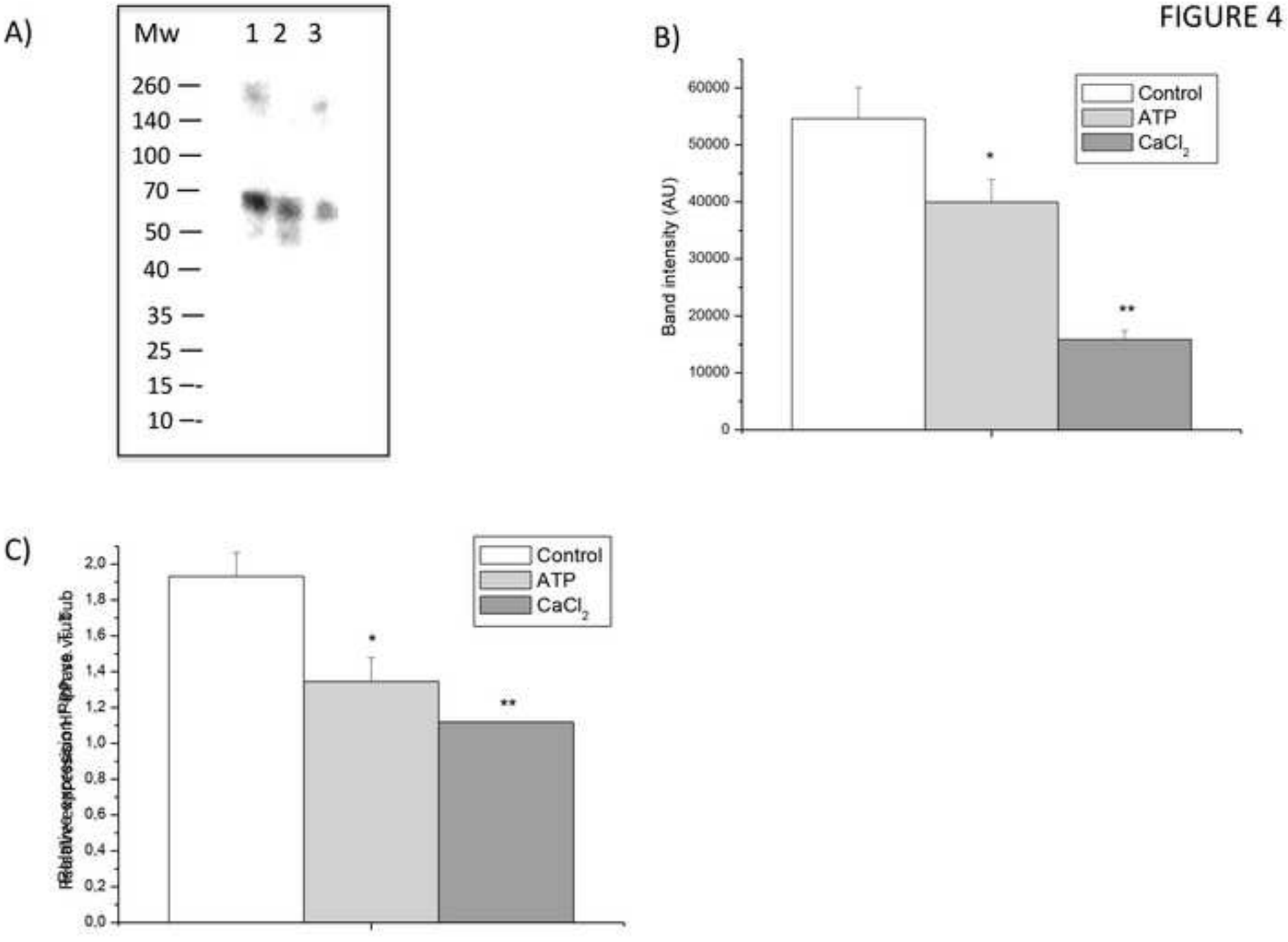

Figure5

Click here to download high resolution image

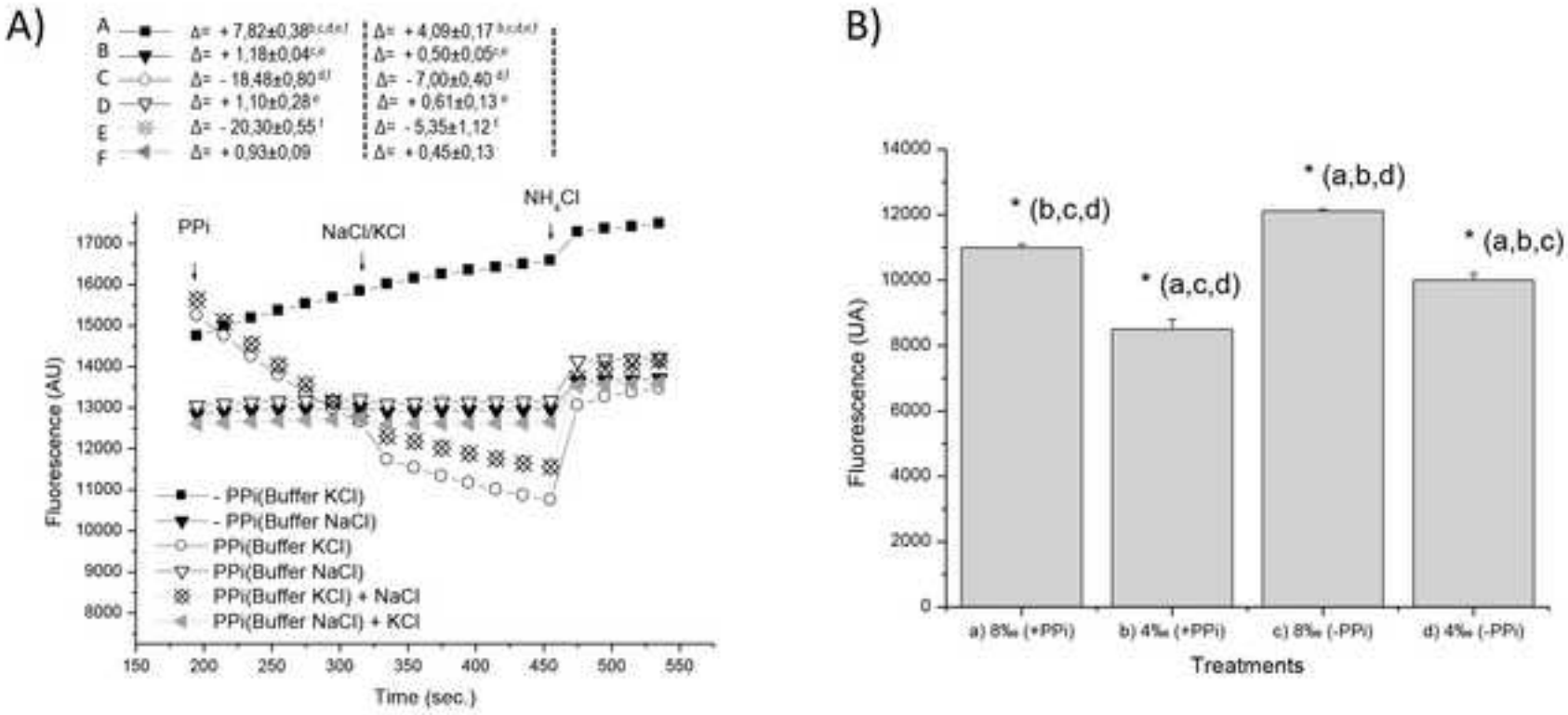

Figure 5